Marian ŁUKANISZYN
Adrian MŁOT

ANALYSIS OF A BLDC MOTOR WITH FRACTIONAL SLOT WINDING

ABSTRACT *This paper presents a three-dimensional analysis of the magnetic field distribution for a three-phase, surface-mounted permanent-magnet, brushless DC motor with integral and fractional slot windings. Calculations are carried out using the 3-D finite element method (FEM). The electromagnetic torque is determined from the co-energy method. It is shown that the ripple-cogging torque can be effectively reduced by an application of the fractional slot-winding. The simulation results are in good agreement with experimental data obtained from the prototype motors.*

Keywords: *brushless DC motors, fractional slot winding, FEM analysis, cogging torque*

1. INTRODUCTION

In the last two decades, permanent-magnet brushless DC (BLDC) motors have been rapidly developed and widely used in various small-size, low-cost drives [1-3]. In such applications, BLDC motors with permanent magnets

Prof. Marian ŁUKANISZYN, D.Sc.
e-mail: luk@po.opole.pl

Adrian MŁOT, M.Sc., Eng.
e-mail: amlot@po.opole.pl

Department of Electrical Engineering and Automatic Control,
Technical University of Opole, Luboszycka 7,
45-036 Opole, POLAND, tel. +(48-77) 4538447

PROCEEDINGS OF ELECTROTECHNICAL INSTITUTE, Issue 229, 2006

appear to be more efficient than induction motors of comparable size. New generations of high-energy permanent magnets enable to obtain magnetic flux densities of 1.0 to 1.2 T in the motor air-gap. This provides high values of the electromagnetic torque developed by the motor. The maximization of the average torque and minimization of the ripple-cogging torque are the most challenging problems in the design and performance of electrical machines [2, 3].

A number of papers have been addressed to the problem of cogging torque reduction. Jahns and Soong [2] have provided an excellent review of pulsating torque minimization techniques for PM motor drives. There are a number of methods, which enable to minimize the cogging torque. Most of them are based on quite complicated modifications of the motor magnetic circuit. One of the most popular techniques to reduce the pulsating torque rely on skewing either the stator lamination stack or rotor magnetization [2, 3]. The skewing decreases variations of the reluctance seen by the rotor magnets, hence reducing the cogging torque. In this paper, it is shown that the ripple-cogging torque can be effectively reduced by an application of the fractional slot-windings.

An effective three-dimensional analysis of the magnetic field distribution for a permanent-magnet brushless DC motor with integral slot-windings has been presented in details by the authors [5, 6]. The simulation results were in good agreement with experimental data obtained from the prototype motor, which confirmed the usefulness of the computational approach. Specifically, the influence of permanent magnet dimensions, air-gap length as well as inhomogeneous magnetization vector on the torque has been comparatively examined [4, 5, 6, 7].

In this paper, the 3-D approach is used to comparatively analyze the magnetic field distribution in the air gap of a BLDC motors with integral and fractional slot windings. It is the authors' experience that the motor construction with fractional slot winding is more efficient than the integral like one, taking into account torque pulsations. Using fractional slot winding is a well-known technique to reduce the high – order back EMF harmonics with some loss of average torque [2].

As the number of slots is not integrally related to the number of poles, the cogging torque is of high frequency and low amplitude. Fractional-slot windings also have good harmonic rejection but do show a significant reduction of the fundamental and thus a reduction of average torque [2]. The designing of multi-phase windings on the base of the 3-phase stators results in producing much cheaper machines but often leads to the fractional slot windings.

The torque ripple in permanent magnet machines can be separated into three components [2]:

1. Cogging torque, caused by the interaction of the permanent magnets' field and stator slotting, which produces reluctance variations with the rotor position. This component is independent of stator current;
2. PM torque ripple, caused by interaction of the PM field with the stator magnetomotive force (MMF) distribution harmonics;
3. Reluctance torque ripple, caused by the interaction between the stator MMF and the angular variation in the rotor magnetic reluctance.

The cogging torque is the main component of the parasitic torques in the motor considered. The main purpose of this study is to reduce the disadvantageous effect of the ripple-cogging torque. For the calculations, professional 3-D FEM software is applied [9]. Two integral quantities calculated from the 3-D model of the real-life prototypes motor with integral and fractional slot windings compare well with the corresponding figures obtained from experimental data.

2. PROTOTYPES OF THE BLDC MOTORS

The prototype motor structure is shown schematically in Fig. 1. The stator is made of laminated iron (sheet type EP 600-50A) and was manufactured by the Besel Company on the base of induction motor Sh80-6.

a) b) c)

Fig. 1. Prototype of the motor (a), cores of stator with integral and fractional windings (b) and rotor with six poles and eight poles for an integral and fractional windings (c)

Structures of the three-phase, double-layer windings (integral and fractional) are presented in Fig. 2. The rotor was made of solid iron with permanent magnets glued to its surface. The permanent magnets have a shape of cylindrical sectors. The motor considered operates as a three-phase brushless DC machine in the auto-piloted mode; thus the rotor speed depends on the value of the load torque. The motor is supplied from a DC source through the

six-pulse electronic inverter. The variable frequency of the supply voltage results from the signals coming from Hall sensors, which indicate the positions of the rotor magnets with regard to the approaching stator poles. The windings are fed with a rectangular current waveform, thus only two phases can be simultaneously supplied. The second quadrant of the B-H characteristic of the permanent magnet type $Nd_2Fe_{14}B$, employed as the flux source for the motor, is linear with a residual flux density B_r of 1.21 T and a coercive magnetizing intensity H_c of – 892 kA/m.

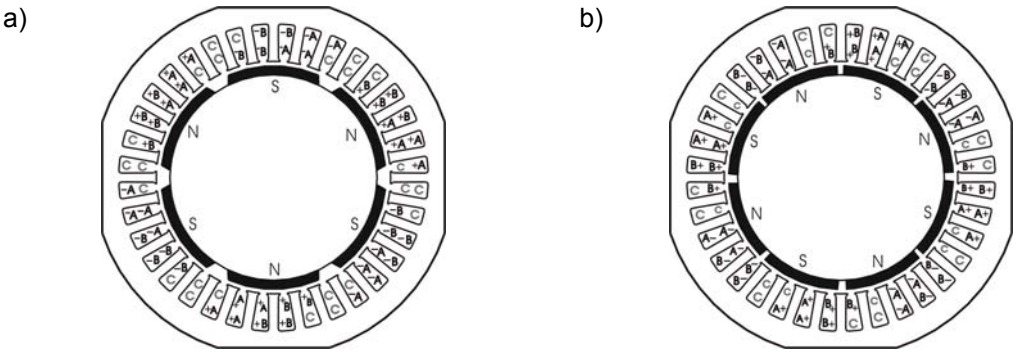

Fig. 2. The BLDC motors a) six poles, q = 2, b) eight poles, q = 3/2

In Table 1 common parameters of BLDC PM motor prototypes with integral and fractional windings are shown.

TABLE 1
Main data of the motor prototypes with integral and fractional windings

	Integral winding	Fractional winding
Air-gap length	1.5 mm	1.5 mm
PM material	sintered NdFeB	sintered NdFeB
PM radial thickness	3 mm	3 mm
Stator outer diameter	60 mm	60 mm
Stator and rotor stack length	59 mm	59 mm
Stator phase resistance	0.34 Ω	1.17 Ω
Arc width of PM pole	47 °	34°
Residual flux density	1.21 T	1.21 T
Coercive magnetizing intensity	892 kA/m^3	892 kA/m^3
Number of rotor poles	2p = 6	2p = 8
Rated Power	0.55 kW	0.25 kW
Rated nominal current	10 A	10 A
Rated nominal voltage	≥ 45 V	≥ 45 V
Max rotational speed	1500 rpm	750 rpm

Diagrams of integral and fractional windings of BLDC PM core are shown in Fig. 3. Fractional windings are called that because the number of slots per pole and phase (q) is not integral.

a) b)

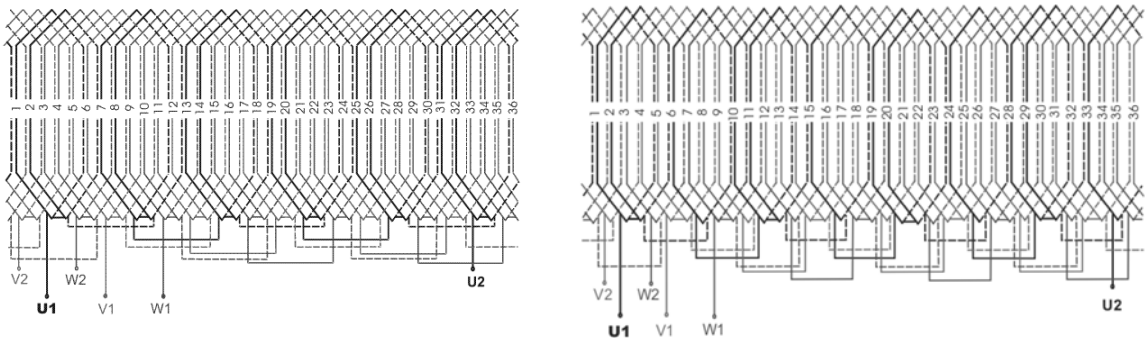

Fig. 3. Diagrams of the three phase double-layer windings a) integral, q = 2 and b) fractional, q = 3/2

3. NUMERICAL MODELS OF THE MOTORS

The motor design requires an accurate knowledge of the magnetic field distribution. The magnetic field derived in the 3-D space allows the determination of the electromagnetic torque, taking into account the 3-D machine structure and the materials the motor is made of. The application of numerical methods enables us to account for non-linearities in the stator and iron cores, demagnetization characteristics of permanent magnets and possible non-uniform distribution of the magnetic field in the machine air gap. The analysis of the magnetic field in 3-D space is performed under the following assumptions:

- The field is considered to be magnetostatic;
- Eddy-currents in construction parts of the motors are omitted;
- Eddy-current losses in rotors are negligible as the permanent magnets rotate together with the rotors;
- The current density within the cross section of the coils is uniform;
- The rotational speed of the motor is constant.

The motor considered has a symmetrical and rotational structure. On the basis of analysis of magnetic fluxes distributions, it is sufficient to limit the

solution to one-sixth part (stator with integral winding) and to one eighth part (stator with fractional winding) of the whole motor volume.

The Flux package uses B-H characteristics to relate flux density and field intensity of all materials. For stator core and the rotor steel, the characteristics are defined in the first quadrant, with the initial values of B and H being both zero. The Flux 3D package was used with specific details presented in [9].

The example of numerical meshed model of the brushless motor with boundary conditions is shown in Fig. 4. In this figure one of three winding phase is presented.

a) b)

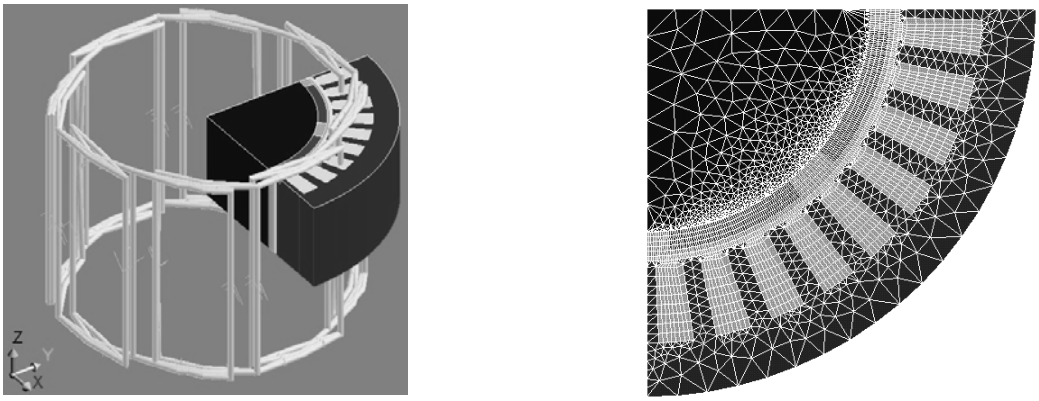

Fig. 4. Numerical model of the BLDC PM motor with fractional winding (a) and calculating mesh (b)

The total numbers of nodes and mesh elements was equal to 72,840 and 134,155, respectively.

The calculation of the electromagnetic torque developed by the motor is performed making use of virtual work method. This method is derived from magnetic co energy (W') changes against space displacement (α). The electromagnetic torque can be calculated by deriving the magnetic co-energy, while maintaining the current constant:

$$T = \left.\frac{\partial W'}{\partial \alpha}\right|_{I=const} \tag{1}$$

where $W' = \int_V \left\{ \int_0^H B \cdot dH' \right\} dV$, α - position angle of the rotor.

The useful ripple-cogging torque factor ε was defined by Nakata at al. [8].

$$\varepsilon = \frac{T_{\max} - T_{\min}}{T_{av}} \cdot 100\,\% \tag{2}$$

where $T_{\max}$, $T_{\min}$, and T_{av} are the maximal, minimal and average values of the torque, respectively.

4. ANALYSIS AND EXPERIMENTAL VALIDATIONS

The calculations have been performed on a PC computer. For both the machine models, the current in the coils was assumed as I = 10 A. Selected calculation results of the magnetic field distribution in the cross-section of BLDC PM motors are presented in Fig. 5.

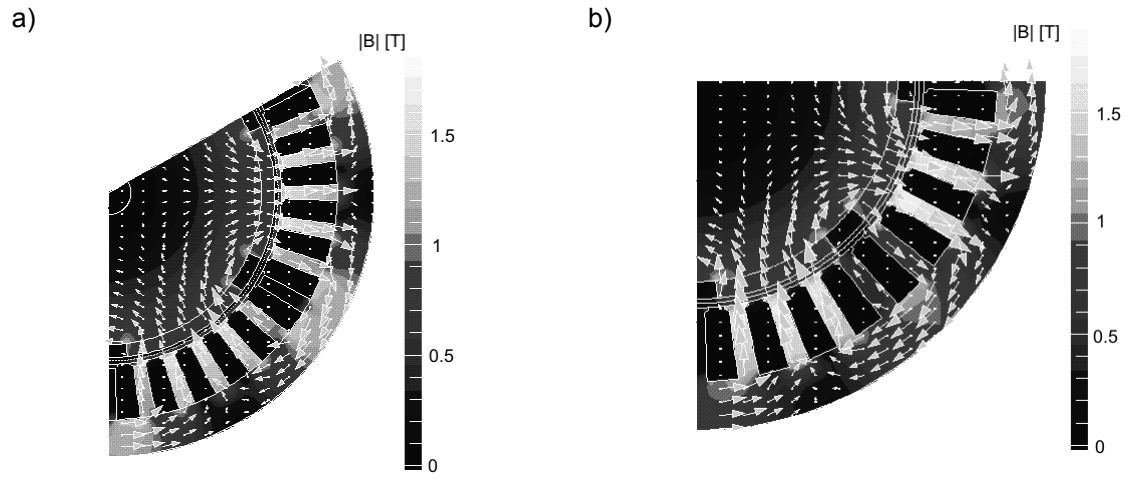

Fig. 5. Simulation result of the flux density distribution for one sixth part of BLDC motor with integral slot winding (a) and one eighth part of BLDC motor with fractional slot winding (b).

Figure 6 compares the electromagnetic and cogging torque predictions obtained by virtual work over surfaces through layer of elements near the magnets, in the center of the air-gap, and near the stator. The comparison of the computed and measured curves is shown.

a) b)

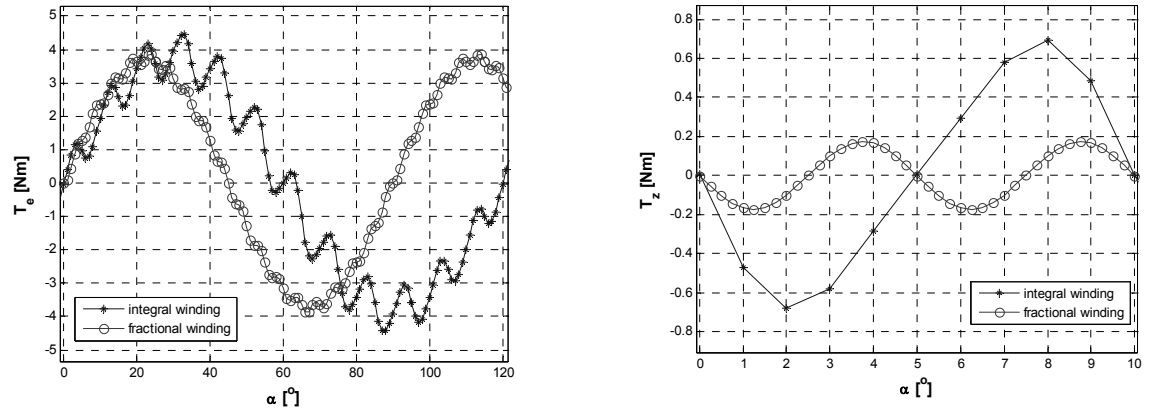

Fig. 6. Electromagnetic torque (a) and cogging torque (b) versus rotor position

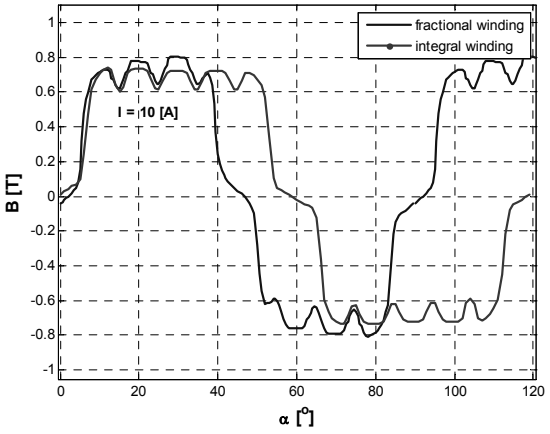

Fig. 7. Flux density in air gap for integral winding and fractional winding versus rotor position

An application of the motor with fractional slot winding allows to obtain less cogging torque from 0.7 Nm to 0.2 Nm after comparing with conventional model of the BLDC PM motor.

Figure 7, 8 and figure 9 present the comparison of the computed results for flux density, flux linkage and back EMF with the measured ones. In table 2, the computed torques for considered versions of the motors are summarized.

a) b)

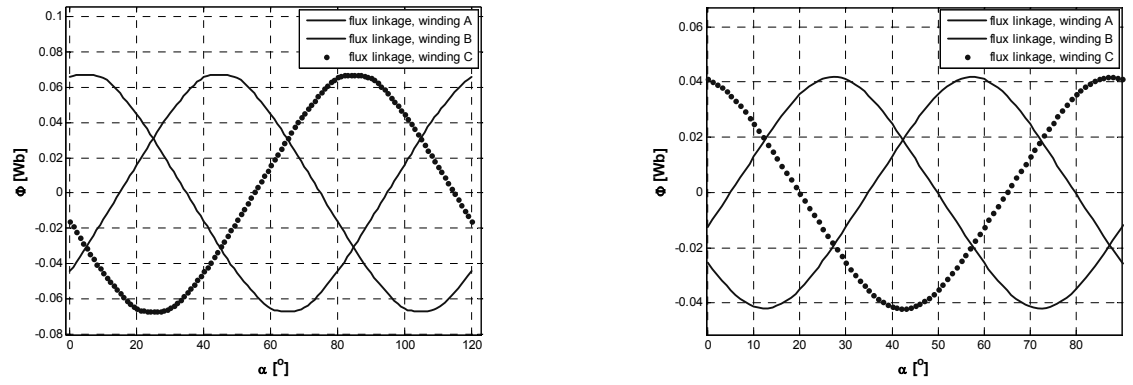

Fig. 8. Flux linkage for integral winding (a) and fractional winding (b) versus rotor position

a) b)

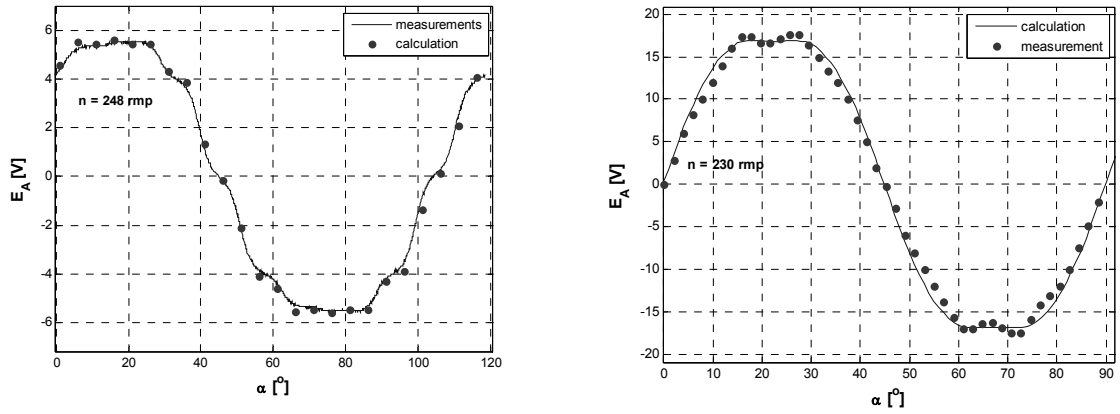

Fig. 9. Back EMF waveform for the integral winding (a) and fractional winding (b)

TABLE 2
Torques of the motor prototypes with integral and fractional windings

Parameter	Integral winding	Fractional winding
ε	76.27 %	21.45 %
$T_{\max}$	4.5 Nm	3.85 Nm
$T_{\min}$	1.9 Nm	3.20 Nm
T_{av}	3.4 Nm	3.03 Nm
T_{cogging}	0.67 Nm	0.2 Nm

5. CONCLUSIONS

This paper presents the computational analysis of PM machines with integral and fractional slot windings. The BLDC PM motor with fractional winding has very high performance regarding low torque ripple and high torque density. The calculations, carried out by 3-D FEM software, are in good agreement with experimental data. Results of the analysis show that application of the fractional winding enables minimization of ripple-cogging torque without decreasing of the average electromagnetic torque.

The cogging torque of PM motor arises from the interaction between rotor magnet and its slotted stator. It has detrimental effects on the motor operation performances, creating speed perturbation, positioning error, vibration, and

noise. Its amplitude is generally dependent on several major factors like shape of stator teeth, slot opening width, air-gap length, pole-arc to pole-pitch ratio of PM, magnets configuration, magnetization distributions and skewing of either stator teeth or magnet pole. More effective solution for cogging torque reduction was used the core of stator with fractional windings.

LITERATURE

1. Glinka T.: *Electrical Machines with permanent magnet (in polish)*, Wydawnictwo Politechniki Śląskiej, Gliwice, 2002.
2. Jahns T.M., Soong W.L.: *Pulsating Torque Minimization Techniques for Permanent Magnet AC Motor Drives – A Review*, IEEE Trans. on Ind. Elect. 43(2), pp.321-330, 1996
3. Kenjo T., Nagamori S.: *Permanent Magnet and Brushless DC Motors, Clarendon Press, Oxford, 1985.*
4. Łukaniszyn M., Młot A.: *Numerical analysis of the brushless permanent motor DC electromagnetic torque and pulsations-components of torque (in polish),* Przegląd Elektrotechniczny, s.21-25, 10'2005.
5. Łukaniszyn M., Młot A.: *Influence of the inhomogeneous magnetization vector on the cogging torque in a brushless DC motor (in polish),* XLII SME'06, Kraków, 2006.
6. Młot A., Łukaniszyn M.: *Influence of the magnetic circuit modifications on the electromagnetic torque in a BLDC motor (in polish),* XI Konferencja Zastosowania Komputerów w Elektrotechnice, s.279-280, 10-12 kwietnia 2006.
7. Młot A., Łukaniszyn M.: *Influence of Halbach magnetization of permanent magnets on a torque in a brushless permanent magnet DC motor, (in polish)*, VII Międzynarodowe Warsztaty Doktoranckie, s. 321-326, Wisła, 2005.
8. Nakata T., Takahashi N., Uehara K.: *Analysis of magnetic characteristics of brush less DC motor taking into account the distribution of magnetization*, IEEE Trans. on Magnetics ,22(5), pp. 1084-1086, 1986.
9. Flux 3D, Cedrat, *User's guide*, volume 2, 2005.

Manuscript submitted 14.11.2006
Reviewed by Krzysztof Kluszczyński

ANALIZA SILNIKA BLDC Z UZWOJENIEM UŁAMKOWYM[*)]

M. ŁUKANISZYN, A. MŁOT[**)]

STRESZCZENIE *W pracy przedstawiono analizę momentu elektromagnetycznego i zaczepowego w silniku bezszczotkowym prądu stałego z magnesami trwałymi (BLDC). Dokonano porównania dwóch prototypów silników z uzwojeniem całkowitym i uzwojeniem ułamkowym (rys. 1). Zastosowanie uzwojenia o ułamkowej liczbie żłobków na biegun i fazę q umożliwia redukcję amplitudy momentu zaczepowego bez konieczności stosowania jakiegokolwiek skosu w obwodzie magnetycznym silnika. Na rysunku 2 pokazano przekroje poprzeczne badanych silników z zaznaczonymi pasmami uzwojenia trójpasmowego. Schemat uzwojenia całkowitego i uzwojenie ułamkowego zamieszczono na rysunku 3. Podstawowe dane konstrukcyjne dotyczącego uzwojenia oraz konstrukcji silnika ujęto w tab. 1.*

Obliczenia polowe przeprowadzono na modelach trój i dwu wymiarowych bazujących na metodzie elementów skończonych. Na rysunku 4 przedstawiono model numeryczny silnika oraz siatkę dyskretyzacyjną przyjętą w obliczeniach.

Rozkłady indukcji magnetycznej w przekrojach silników z uzwojeniem całkowitym oraz uzwojeniem ułamkowym pokazano na rys. 5. Obliczenia momentu elektromagnetycznego wykonano za pomocą metody pracy wirtualnej według zależności (1). Wyniki obliczeń momentu elektromagnetycznego, momentu zaczepowego (rys. 6), siły elektromotorycznej indukowanej w poszczególnych pasmach (rys. 9), indukcji magnetycznej w szczelinie maszyny (rys. 7) oraz strumieni skojarzonych (rys. 8) zweryfikowano częściowo pomiarami na prototypach maszyn. W tabeli 2 zestawiono wyniki obliczeń momentów elektromagnetycznego i zaczepowego. W celu określenia pulsacji momentu elektromagnetycznego, ujęto w tabeli również współczynnik pulsacji, przyjęty za Nakatą według wzoru (2).

Przedstawiona analiza i obliczenia potwierdzają możliwości minimalizacji momentu zaczepowego w silnikach z uzwojeniami ułamkowymi.

[*)] *Praca zrealizowana w ramach grantu promotorskiego MNiI Nr 3T10A03129 i jest współfinansowana ze środków EFS oraz ze środków budżetu państwa.*

[**)] Mgr inż. **A. Młot** jest stypendystą Europejskiego Funduszu Społecznego (EFS).